Supplementary Information

Location of Stimuli-Responsive Peptide Sequences within Silk-Elastinlike Protein-Based Polymers Affects Nanostructure Assembly and Drug-polymer Interactions

Kyle J. Isaacson[1,2], M. Martin Jensen[1,2], Douglas B. Steinhauff[1,2], James E. Kirklow[2], Raziye Mohammadpour[1], Jason W. Grunberger[1,3], Joseph Cappello[3], Hamidreza Ghandehari[1,2,3]

[1]Utah Center for Nanomedicine, Nano Institute of Utah, University of Utah, Salt Lake City, UT, USA

[2]Department of Biomedical Engineering, University of Utah, Salt Lake City, UT, USA

[3]Department of Pharmaceutics and Pharmaceutical Chemistry, University of Utah, Salt Lake City, UT, USA

Tables

Table S1. Goodness-of-fit values (R^2-values) for various drug release models to the obtained dataset for the first six hours of doxorubicin release in the experimental microdialysis setup.

Sample and MMP Concentration	**Zero-Order**	**First-Order**	**Weibull**	**Higuchi**	**Hixson-Crowell**	**Korsmeyer-Peppas**
DOX 0 nM	0.935801	0.992898	0.856573	0.930835	0.990817	0.887476
DOX 1 nM	0.941233	0.988214	0.831934	0.923659	0.993147	0.912958
DOX 5 nM	0.948555	0.981058	0.800255	0.929939	0.995676	0.945814
DOX 50 nM	0.933161	0.995909	0.860358	0.942723	0.992407	0.941734

Table S2. Goodness-of-fit values (R^2-values) for various drug release models to the obtained datasets for 6-96 hours of doxorubicin release from various SELP formulations in differing concentrations of active MMP-9.

Sample and MMP Concentration	**Zero-Order**	**First-Order**	**Weibull**	**Higuchi**	**Hixson-Crowell**	**Korsmeyer-Peppas**
815K 0 nM	0.741341	0.803655	0.987178	0.865898	0.783452	0.919525
815K 1 nM	0.774016	0.834759	0.993518	0.891578	0.815256	0.940034
815K 5 nM	0.840429	0.898353	0.998852	0.937049	0.880085	0.963743
815K 50 nM	0.802826	0.864680	0.998908	0.912878	0.844931	0.952313
815K-RS1 0 nM	0.838295	0.874982	0.992791	0.934605	0.863043	0.978882
815K-RS1 1 nM	0.729115	0.759910	0.965288	0.853000	0.749713	0.929653
815K-RS1 5 nM	0.831667	0.856944	0.991038	0.929560	0.848706	0.975373
815K-RS1 50 nM	0.816466	0.857705	0.997438	0.922065	0.844383	0.971873
815K-RS2 0 nM	0.793393	0.888290	0.999447	0.903403	0.858896	0.940866
815K-RS2 1 nM	0.831945	0.921480	0.993919	0.931348	0.894510	0.960161
815K-RS2 5 nM	0.826386	0.907495	0.998212	0.927258	0.882557	0.956808
815K-RS2 50 nM	0.780241	0.870528	0.999276	0.894457	0.842208	0.935808

Figures

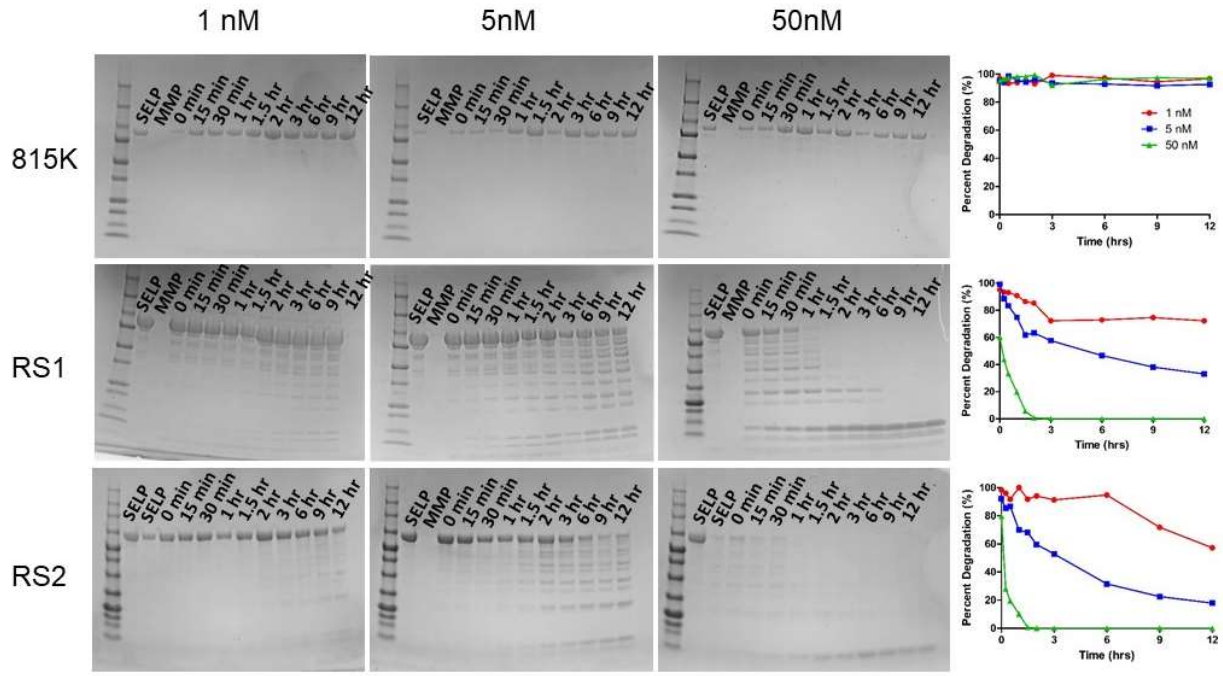

Figure S1. Acrylamide gels showing the degradation of SELPs 815K, 815K-RS1, and 815K-RS2 following incubation at 37 °C at various time points (0-12 hrs) with active MMP-9 at concentrations of 1 nM, 5 nM, and 50 nM. Degradation plots as determined via ImageJ analysis of the various acrylamide gel images.

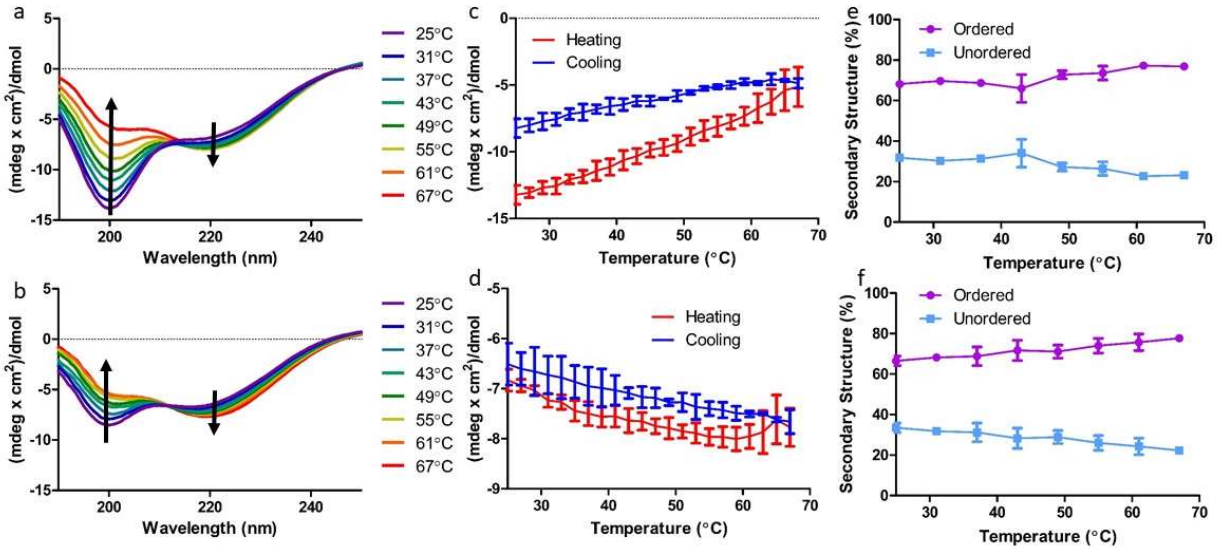

Figure S2. Secondary structure analysis of SELP 815K-RS1 via circular dichroism spectropolarimetry. (a) CD spectra upon heating from 25 to 67 °C. (b) CD spectra upon cooling from 67 to 25 °C, (c) ellipticity peak values at 198 nm, (d) ellipticity peak values at 220 nm, and (e) percentages of ordered and unordered secondary structures – as determined by CDSSTR spectral deconvolution – upon heating and (f) cooling.

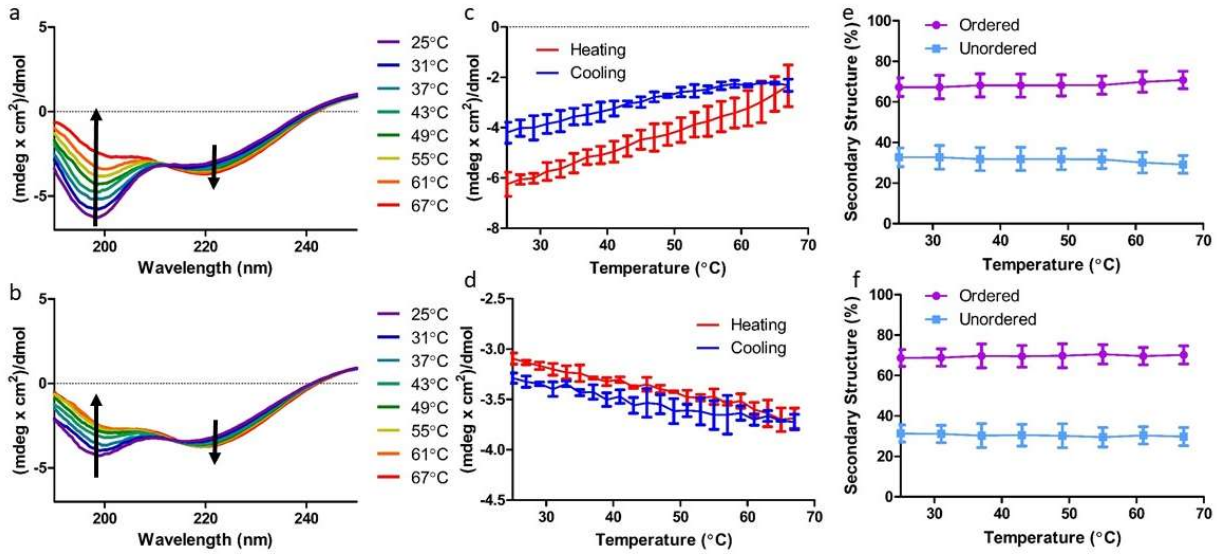

Figure S3. Secondary structure analysis of SELP 815K-RS2 via circular dichroism spectropolarimetry. (a) CD spectra upon heating from 25 to 67 °C, (b) CD spectra upon cooling from 67 to 25 °C, (c) ellipticity peak values at 198 nm, (d) ellipticity peak values at 220 nm, and (e) percentages of ordered and unordered secondary structures – as determined by CDSSTR spectral deconvolution – upon heating and (f) cooling.

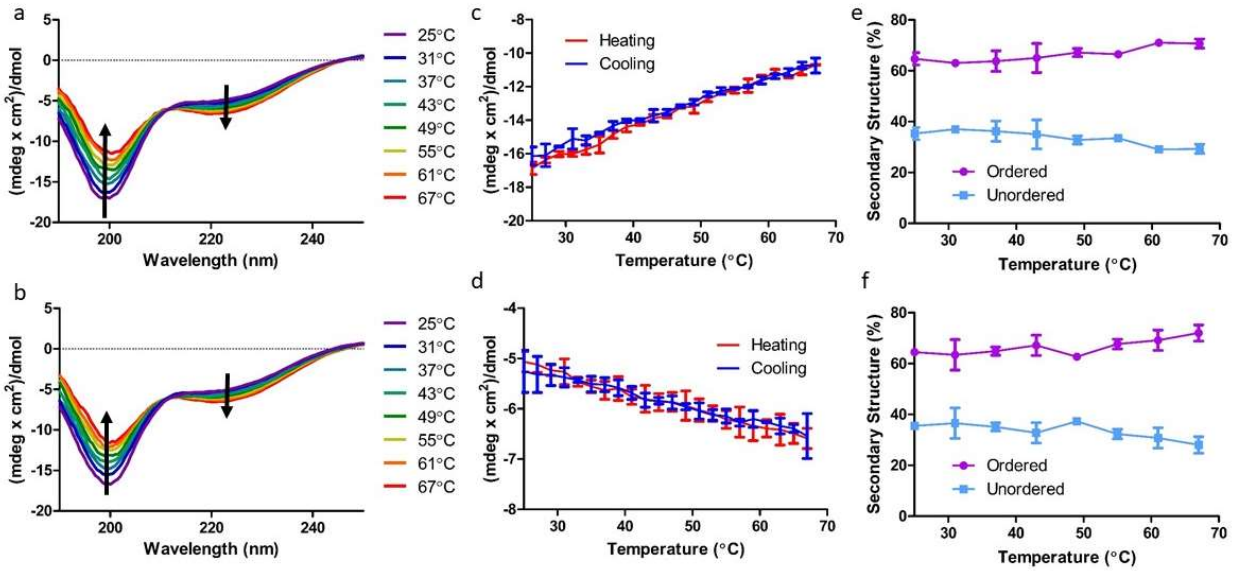

Figure S4. Secondary structure analysis of SELP 815K-RS5 via circular dichroism spectropolarimetry. (a) CD spectra upon heating from 25 to 67 °C, (b) CD spectra upon cooling from 67 to 25 °C, (c) ellipticity peak values at 198 nm, (d) ellipticity peak values at 220 nm, and (e) percentages of ordered and unordered secondary structures – as determined by CDSSTR spectral deconvolution – upon heating and (f) cooling.

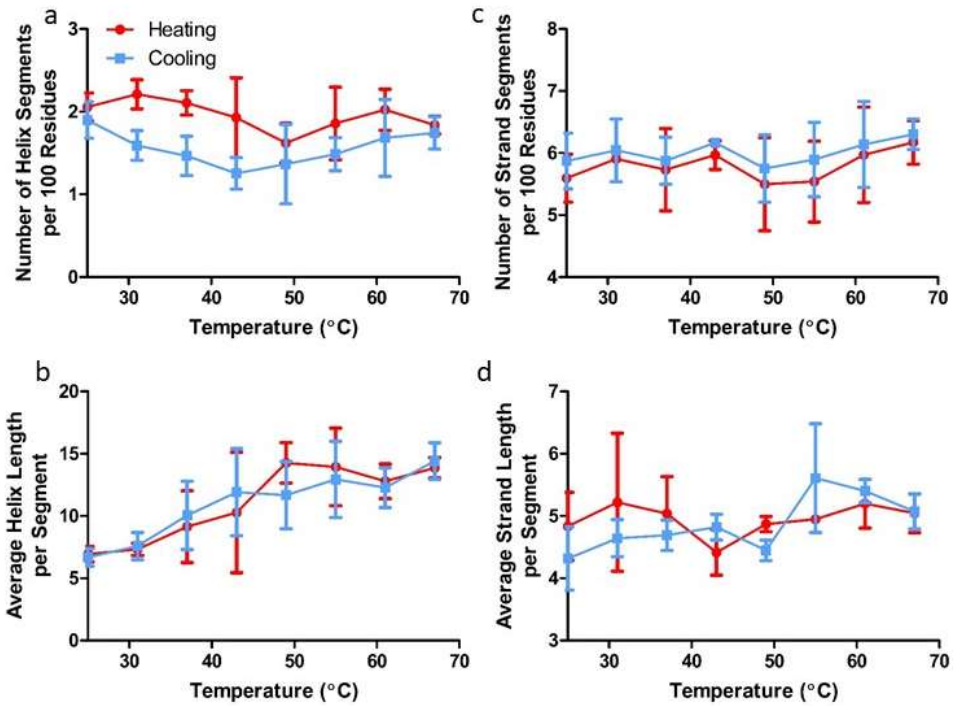

Figure S5. Changes to number and length of protein helix and strand structure of SELP 815K-RS1 as determined by CDSSTR spectral deconvolution over a temperature range of 25-67 °C. (a) Number of helix segments per 100 residues, (b) average helix length per segment, (c) number of strand segments per 100 residues, and (d) average strand length per segment.

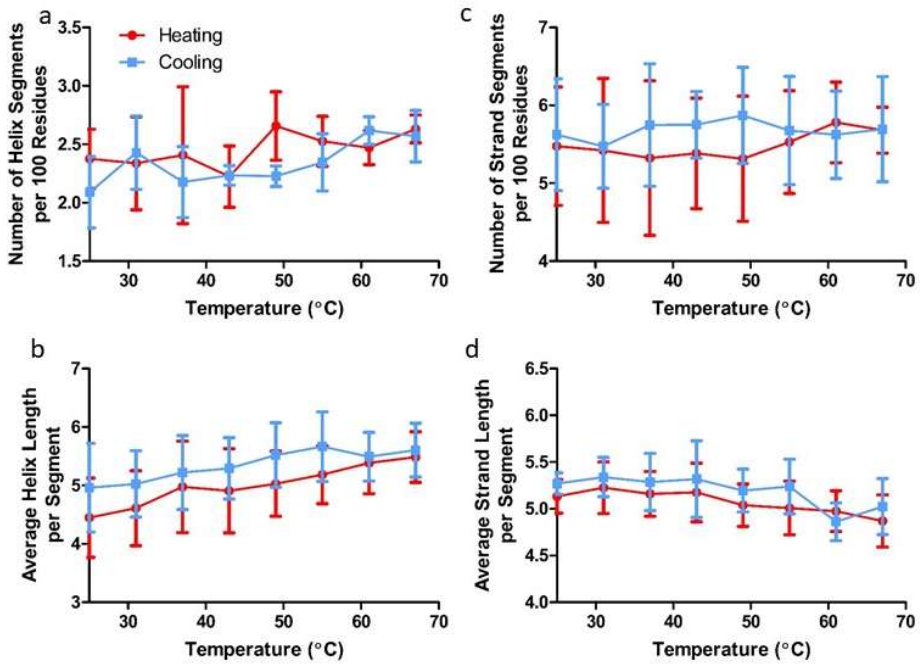

Figure S6. Changes to number and length of protein helix and strand structure of SELP 815K-RS2 as determined by CDSSTR spectral deconvolution over a temperature range of 25-67 °C. (a) Number of helix segments per 100 residues, (b) average helix length per segment, (c) number of strand segments per 100 residues, and (d) average strand length per segment.

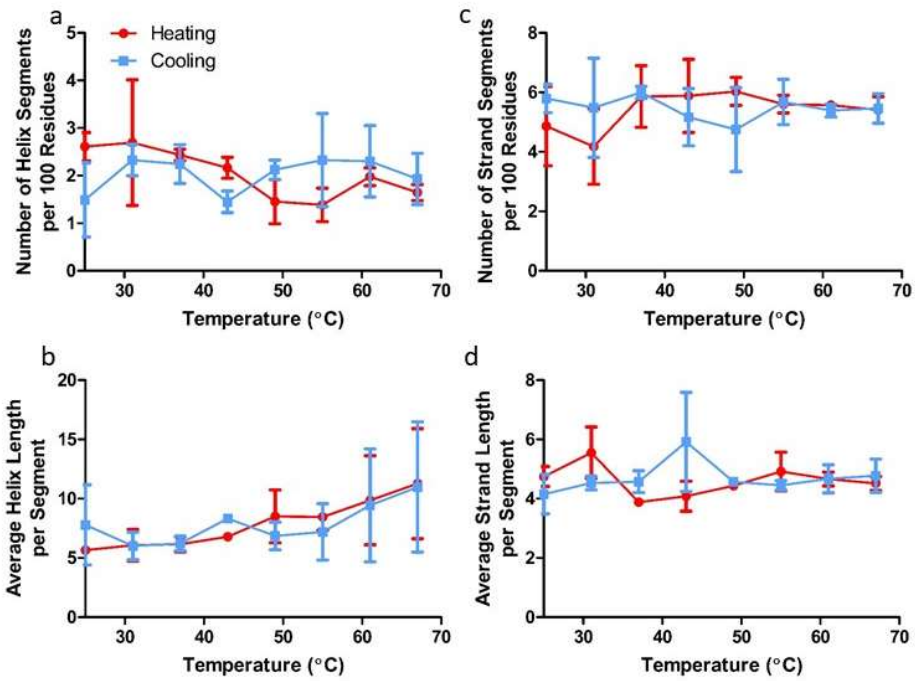

Figure S7. Changes to number and length of protein helix and strand structure of SELP 815K-RS5 as determined by CDSSTR spectral deconvolution over a temperature range of 25-67 °C. (a) Number of helix segments per 100 residues, (b) average helix length per segment, (c) number of strand segments per 100 residues, and (d) average strand length per segment.

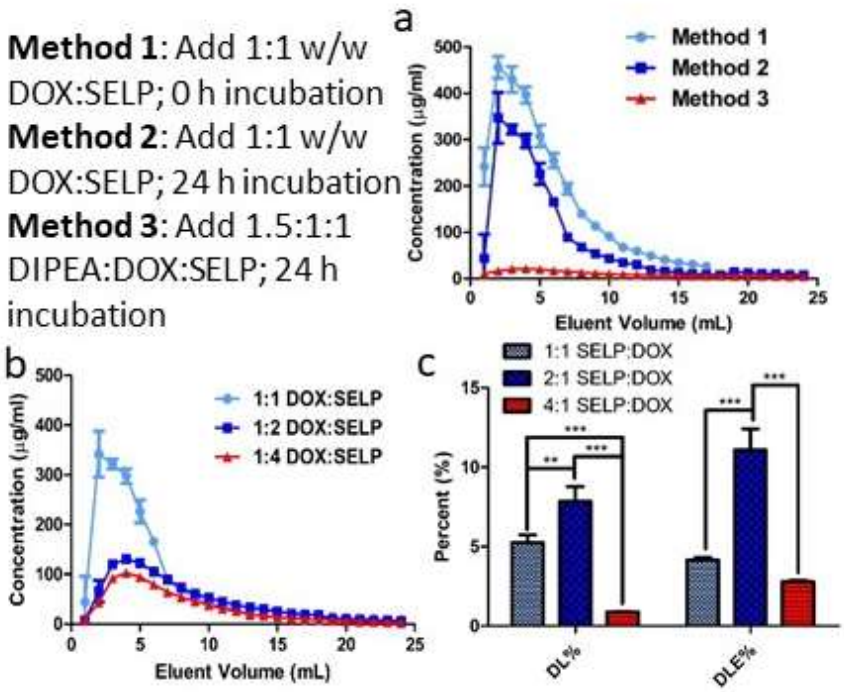

Figure S8. Optimization of DOX loading parameters within SELP 815K nanoassemblies. (a) DOX concentration in the eluent vs. elution volume for the various methods utilized to load DOX into SELP 815K nanoassemblies. (b) DOX concentration in the eluent vs. elution volume for SELP 815K nanoassemblies when co-incubated with DOX at different ratios. (c) Drug loading and drug loading efficiency percentages for SELP 815K co-incubated with DOX at different ratios.

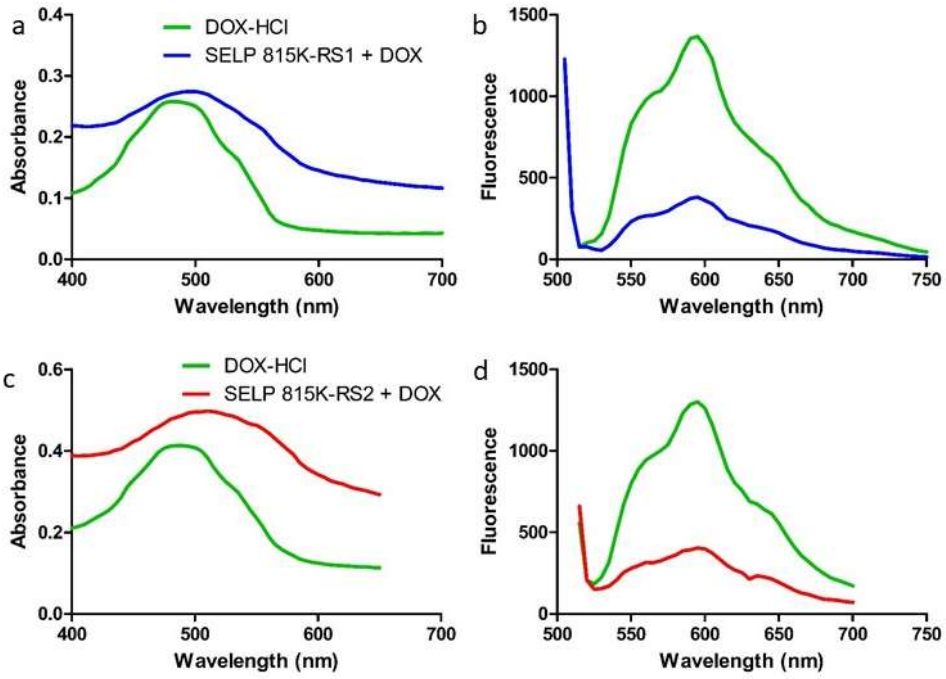

Figure S9. Changes in DOX absorbance and fluorescence following loading into SELPs 815K-RS1 and 815K-RS2. (a) Absorbance and (b) fluorescence spectra of DOX-HCl and DOX-loaded SELP 815K-RS1. (c) Absorbance and (d) fluorescence spectra of DOX HCl and DOX-loaded SELP 815K-RS2. Native absorbance and fluorescence of the SELPs were negligible.

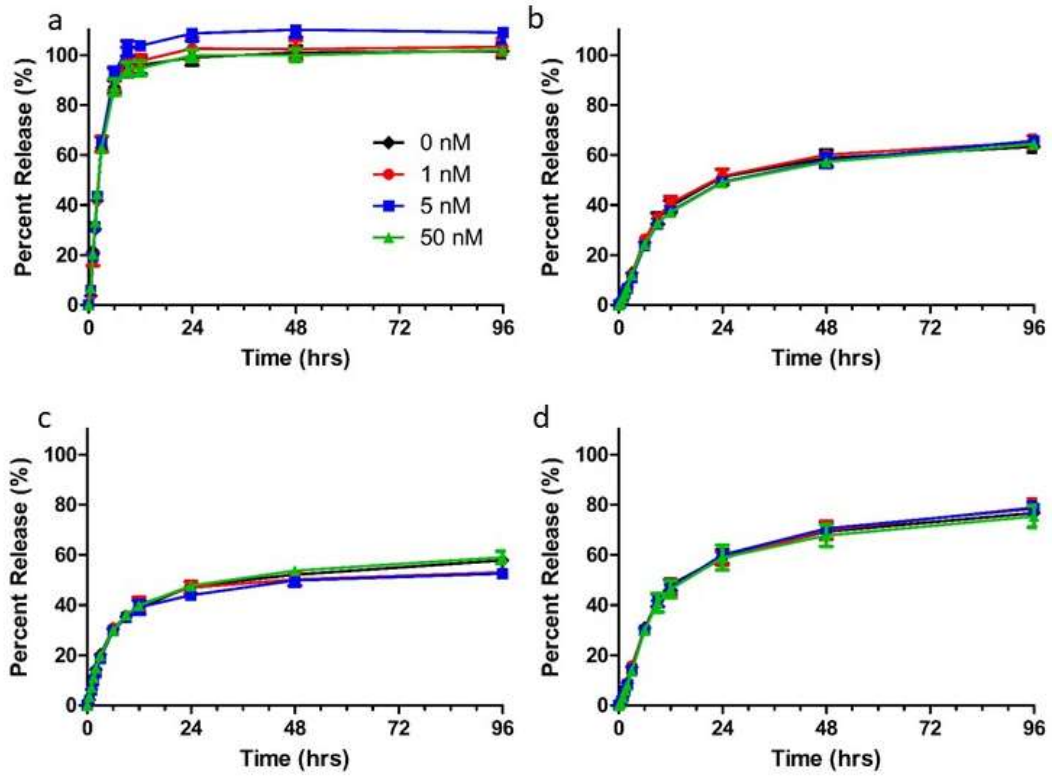

Figure S10. Release of DOX across a microdialysis setup from (a) no vehicle, (b) SELP 815K, (c) SELP 815K-RS1, and (d) SELP 815K-RS2 in various concentrations of MMP-9: 0 nM, 1 nM, 5 nM, and 50 nM. The DOX sample refers to the passage of free DOX across the microdialysis membrane and into the measured reservoir.

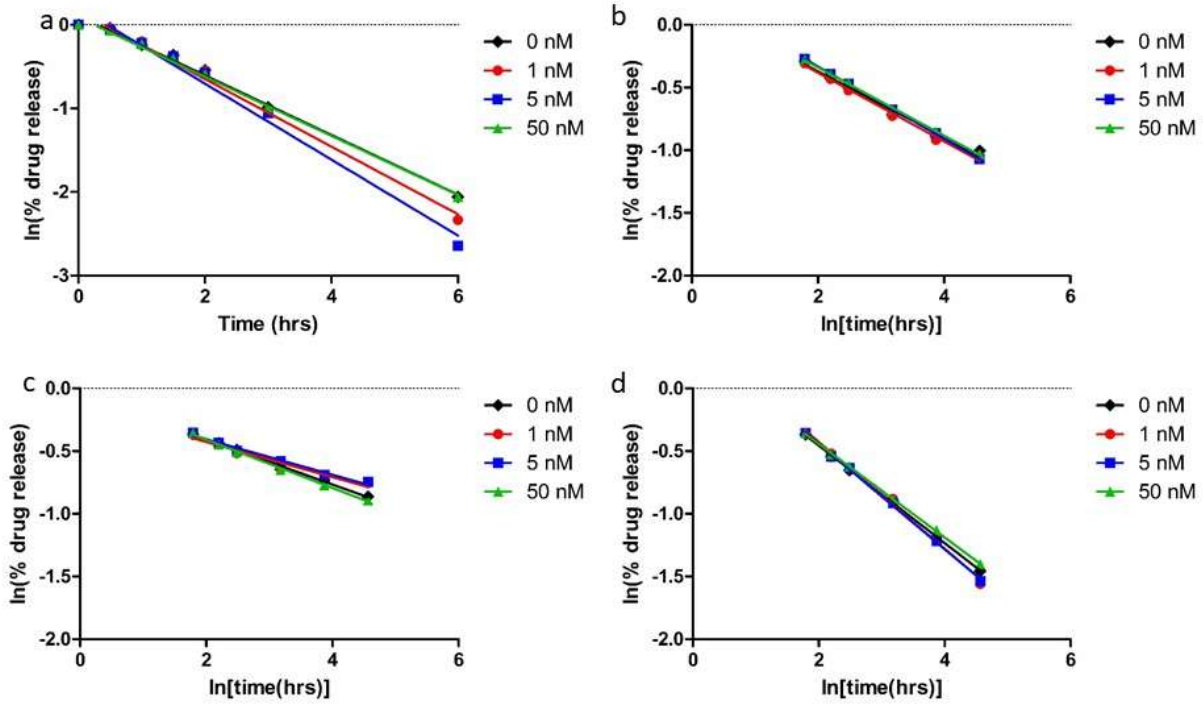

Figure S11. Modeling of DOX release profiles in varying MMP-9 concentrations. (a) First-order release model of free DOX passing across the microdialysis setup from 0-6 hrs. (b) Weibull release model of DOX from SELP 815K from 6-96 hrs. (c) Weibull release model of DOX from SELP 815K-RS1 from 6-96 hrs. (d) Weibull release model of DOX from SELP 815K-RS2 from 6-96 hrs.